

Immersing carbon nanotubes in cold atomic gases

C. T. Wei^{1,2}, P. V. Mironova,³ J. Fortágh,¹ W. P. Schleich,² and R. Walser^{3,*}

¹Physikalisches Institut, Eberhard-Karls-Universität Tübingen, D-72076 Tübingen, Germany

²Institut für Quantenphysik and Center for Integrated Quantum Science and Technology (IQST), Universität Ulm, D-89069 Ulm, Germany

³Institut für Angewandte Physik, TU Darmstadt, D-64289 Darmstadt, Germany

(Received 8 July 2013; published 17 October 2013)

We investigate the sympathetic relaxation of a free-standing, vibrating carbon nanotube that is mounted on an atom chip and is immersed in a cloud of ultracold atoms. Gas atoms colliding with the nanotube excite phonons via a Casimir-Polder potential. We use Fermi's golden rule to estimate the relaxation rates for relevant experimental parameters and develop a fully dynamic theory of relaxation for the multimode phononic field embedded in a thermal atomic reservoir. Based on currently available experimental data, we identify the relaxation rates as a function of atom density and temperature that are required for sympathetic ground-state cooling of carbon nanotubes.

DOI: [10.1103/PhysRevA.88.043623](https://doi.org/10.1103/PhysRevA.88.043623)

PACS number(s): 67.85.-d, 07.10.Cm, 85.35.Kt, 34.35.+a

I. INTRODUCTION

In 1959, Richard Feynman gave the visionary talk “There's Plenty of Room at the Bottom” [1] and drew the road map for the coming quantum technologies. Half a century later, we are still amid the silicon era and enjoy many gadgets based on lithographically manufactured nanoelectronics. In terms of miniaturization, many sectors of nanotechnology [2] have reached the proverbial quantum bottom, but today, this milestone is recognized rather as a resource for novel devices [3,4] than the ultimate limit.

Currently, there are many activities [4,5] to combine well-characterized individual quantum systems, like trapped ions [6,7], degenerate quantum gases [8], superfluid or superconducting Josephson junctions [9], quantum dots [10], and nanomechanical oscillators [11–13], with microwave guides, optical resonators, and fibers [14], to form hybrid quantum systems. Possible applications of such systems range from high-precision force and mass measurements to quantum computation [15–19].

In this context, carbon nanotubes [20,21] are a particularly promising form of rolled-up, monolayered carbon sheets. These families of fullerenes [22] combine fascinating aspects of electrical conductivity, exceptional mechanical tension moduli with the ability to be grown on demand or to be deposited mechanically on atomic chips [23–25]. Such features render carbon nanotubes on atom chips ideal candidates to explore quantum-mechanical limits [11,13,26,27], to construct single-atom detectors [28] with them, or to hybridize them with matter waves [29].

Polarizable particles in front of surfaces are affected by Casimir-Polder potentials [30–32]. The measurement of such minute forces with ultracold atoms is of high interest [33–36]. In particular, the interaction and trapping of atoms in front of nanotubes has been explored [37,38]. However, so far only a few experiments have been performed with carbon nanotubes immersed in ultracold alkali-metal gases [29,39].

In this article, we will combine aspects of the quantum motion of carbon nanotubes and the quantum degeneracy of the matter waves to examine the prospects for the sympathetic

cooling due to the Casimir-Polder interaction of a free-standing carbon nanotube mounted on an atom chip. In Sec. II, we discuss a micromechanical model of the oscillating carbon nanotube and quantize the phononic excitations. We introduce the energies of the atomic gas, phonons, and the atom-phonon interaction. Within the Heisenberg picture, we model the temporal evolution and obtain equilibrium relaxation rates versus the temperature for different densities of the atomic cloud in Sec. III. This approach is generalized in Sec. IV, where we formulate a fully dynamical theory for the density operator of the phonons. We conclude the theoretical analysis with a numerical study of the cooling efficiency of a carbon nanotube due to the interaction with the cold atoms. Two short Appendices summarize properties of the carbon nanotubes and thermodynamic correlation functions for degenerate bosonic gases.

II. ATOMS HITTING CARBON NANOTUBES

In the present section, we will introduce the basic mechanical features of single-walled carbon nanotubes. In particular, we will consider the experimental setup of Schneeweiss *et al.* [29], where free-standing carbon nanotubes are grown on an atomic chip [23,25] and interact with ultracold atoms in ultrahigh-vacuum systems.

From a continuum model of a free-standing carbon nanotube, we derive a quantized description of the phononic excitations. This carbon nanotube is embedded in an ultracold atomic bosonic gas at temperatures above the critical temperature for Bose-Einstein condensation (BEC). In particular, we model the interaction between a carbon nanotube and a ⁸⁷Rb alkali atom by a Casimir-Polder interaction potential [29]. This approach leads to a total energy for the carbon nanotube immersed in an atomic bath.

A. Vibrating carbon nanotube

The vibrations of a carbon nanotube can be well described by the Euler-Bernoulli model of an oscillating beam [13,20,40,41]. Here, we use a real, transversal displacement field $\mathbf{u}(z,t) \equiv u_x(z,t)\mathbf{e}_x + u_y(z,t)\mathbf{e}_y$ to represent the two-dimensional bending of an elastic beam of length L , which is aligned along the surface normal (z axis) of an atomic chip. The transverse polarization directions are denoted \mathbf{e}_x

*Reinhold.Walser@physik.tu-darmstadt.de

and \mathbf{e}_y . To be precise, we have to specify the boundary conditions $\mathbf{u}(0,t) = \partial_z \mathbf{u}(0,t) = 0$ for the fixed end on the chip and $\partial_z^2 \mathbf{u}(L,t) = \partial_z^3 \mathbf{u}(L,t) = 0$ on the loose end.

In the case of small displacements, the vibration of the tube follows from the linear Euler-Bernoulli equation

$$(\rho_c \partial_t^2 + EI \partial_z^4) \mathbf{u}(z,t) = 0. \quad (1)$$

The physical parameters are [41–43] the linear mass density ρ_c (kg/m), the Young's modulus E (Pa), and the area moment of inertia I (m⁴).

The general solution of Eq. (1) can be written as

$$\mathbf{u}(z,t) = \frac{1}{\sqrt{2}} \sum_{\substack{l=0 \\ \sigma=x,y}}^{\infty} \mathbf{e}_\sigma \phi_l(z) (e^{-i\omega_l t} \beta_{l\sigma} + e^{i\omega_l t} \beta_{l\sigma}^*) \quad (2)$$

if we can determine the eigenfrequencies ω_l and the phononic eigenmodes $\phi_l(z)$ of the problem. From the axial symmetry of Eq. (1), it follows that the transverse oscillation frequencies must be degenerate for both polarization directions. The complex amplitudes $\beta_{l\sigma}$ are determined from the initial conditions.

This model of an oscillating beam, together with the boundary conditions, leads to a self-adjoint eigenvalue problem for the modes with respect to the real scalar product,

$$\langle \phi_l | \phi_m \rangle \equiv \int_0^L \frac{dz}{L} \phi_l(z) \phi_m(z) = a_l^2 \delta_{l,m}. \quad (3)$$

Explicitly, the eigenmodes read

$$\begin{aligned} \phi_l(z) = & \tilde{a}_l [(\cos \kappa_l L + \cosh \kappa_l L)(\cos \kappa_l z - \cosh \kappa_l z) \\ & + (\sin \kappa_l L + \sinh \kappa_l L)(\sin \kappa_l z - \sinh \kappa_l z)], \end{aligned} \quad (4)$$

where the normalization constants \tilde{a}_l , defined by Eq. (A1), are proportional to the harmonic oscillator length $a_l \equiv \sqrt{\hbar/\omega_l \rho_c L}$.

However, a mechanical oscillation is only possible if the wave numbers κ_l satisfy the condition

$$\cos(\kappa_l L) \cosh(\kappa_l L) = -1. \quad (5)$$

At first glance, the solution of this equation looks like a formidable task, but in fact the phononic wave numbers can be approximated quite well [27] by an equidistant array $\kappa_l \cong \pi(l + 1/2)/L$ for $l \geq 0$.

From the solution of Eq. (1), we obtain finally the particle-like dispersion relation,

$$\omega_l = \sqrt{\frac{EI}{\rho_c}} \kappa_l^2, \quad (6)$$

for the phononic frequency ω_l of mode l . Such a quadratic phonon dispersion relation can be derived also microscopically from the zone-folding method [44], considering the lattice symmetries of graphene [27].

Having determined the eigenmodes of the tube, we represent the energy of the phonon field,

$$\begin{aligned} H_c & \equiv \int_0^L dz \left[\frac{\rho_c}{2} (\partial_t \mathbf{u})^2 + \frac{EI}{2} (\partial_z^2 \mathbf{u})^2 \right] \\ & = \sum_{\substack{l=0 \\ \sigma=x,y}}^{\infty} \hbar \omega_l \beta_{l\sigma}^* \beta_{l\sigma}, \end{aligned} \quad (7)$$

as a separable sum of independent oscillator modes, which is necessary for the quantization of the phononic field,

$$\hat{\mathbf{u}}(z) = \frac{1}{\sqrt{2}} \sum_{\substack{l=0 \\ \sigma=x,y}}^{\infty} \mathbf{e}_\sigma \phi_l(z) (\hat{b}_{l\sigma} + \hat{b}_{l\sigma}^\dagger), \quad (8)$$

in terms of bosonic excitations $[\hat{b}_{l\sigma}, \hat{b}_{l'\sigma'}^\dagger] = \delta_{ll'} \delta_{\sigma\sigma'}$, acting on the multimode phononic Fock-states $|\dots, n_{l\sigma}, \dots\rangle$.

Thus, we obtain the Hamiltonian operator

$$\hat{H}_c = \sum_{\substack{l=0 \\ \sigma=x,y}}^{\infty} \hbar \omega_l \hat{b}_{l\sigma}^\dagger \hat{b}_{l\sigma} \quad (9)$$

of the vibrating carbon nanotube.

B. Cold atomic gas

Atoms colliding with the carbon nanotube are modeled as a homogeneous gas of scalar bosons represented in a discrete plane-wave basis as $[\hat{a}_{\mathbf{k}}, \hat{a}_{\mathbf{k}'}^\dagger] = \delta_{\mathbf{k}\mathbf{k}'}$. This representation implies periodic boundary conditions for all spatial fields, e.g., the atomic field $\hat{\Psi}(\mathbf{r} + \mathbf{e}_i L_i) = \hat{\Psi}(\mathbf{r})$, where L_x , L_y , and L_z are the lengths of the quantization box.

Normalized plane waves $\langle \mathbf{r} | \mathbf{k} \rangle \equiv \exp(i\mathbf{k} \cdot \mathbf{r})/\sqrt{\mathcal{V}}$ are then a complete set of basis functions within the quantization volume $\mathcal{V} \equiv L_x L_y L_z$. For the length of the quantization volume in the z direction, we choose the length $L_z = L$ of the carbon nanotube.

This spatial periodicity leads to a discrete set of atomic wave vectors $k_i = 2\pi n_i/L_i$, $n_i \in \mathbb{Z}$. Hence, we obtain for the spatial amplitude of the atomic field the expression

$$\hat{\Psi}(\mathbf{r}) = \sum_{\mathbf{k}} \langle \mathbf{r} | \mathbf{k} \rangle \hat{a}_{\mathbf{k}}, \quad (10)$$

and the density of the atomic gas follows as

$$\hat{n}(\mathbf{r}) \equiv \hat{\Psi}^\dagger(\mathbf{r}) \hat{\Psi}(\mathbf{r}) = \sum_{\mathbf{k}, \mathbf{q}} \hat{a}_{\mathbf{q}}^\dagger \hat{a}_{\mathbf{k}} \langle \mathbf{r} | \mathbf{k} \rangle \langle \mathbf{q} | \mathbf{r} \rangle. \quad (11)$$

In this article, we consider atomic temperatures above the Bose-Einstein condensation temperature, where corrections to the ideal gas energy are minute. Therefore, we only keep in the energy the kinetic energy,

$$\hat{H}_a \equiv \sum_{\mathbf{k}} \varepsilon_{\mathbf{k}} \hat{a}_{\mathbf{k}}^\dagger \hat{a}_{\mathbf{k}}, \quad \varepsilon_{\mathbf{k}} \equiv \frac{\hbar^2 \mathbf{k}^2}{2m} = \hbar \omega_{\mathbf{k}}, \quad (12)$$

of the gas.

C. Casimir-Polder potential

The interaction of a neutral, polarizable atom in front of a surface is described by the Casimir-Polder theory [31,32, 37,45–47]. In principle, a full three-dimensional geometric modeling of the Casimir-Polder potential surface would be in place to describe all details of the interaction. However, we assume for simplicity that the dominant contribution to the dynamics is obtained by the axis-symmetric, translationally invariant part of the Casimir-Polder potential $V(\mathbf{r}) = V(\rho)$,

where $\rho \equiv \sqrt{x^2 + y^2}$ is the radius in cylindrical coordinates with the z axis oriented along the tube.

Recent experiments [29,36] have provided evidence that the dominant contribution is given by an inverse power-law term $\sim C_5/\rho^5$. However, in order to keep the model flexible, we approximate the Casimir-Polder potential as an inverse power series,

$$V(\rho) = \sum_{n=n_m}^{\infty} \frac{C_n}{\rho^n}, \quad (13)$$

for distances well above the tube's physical radius $\rho > R$. For example, in the case of a single-walled carbon nanotube $R = 1$ nm.

The different contributions to the short-range part of the potential are parameterized by real coefficients C_n , starting at least with terms beyond $n_m > 2$. The surface physics (adhesion or adsorption) at $\rho = R$ is unknown but should be of no concern for the calculation of the collisional relaxation. Thus, we assume that the potential is real and vanishes within the tube $V(\rho \leq R) = 0$.

The later analysis requires the Fourier transform

$$V_{\mathbf{q}} \equiv \int_{\mathcal{V}} d^3r \langle \mathbf{q} | \mathbf{r} \rangle V(\mathbf{r}) = \frac{\delta_{q_z,0}}{\sqrt{\mathcal{V}}} L V(q) \quad (14)$$

of the Casimir-Polder potential, where $V(q)$ is the two-dimensional, axis-symmetric Fourier transform of the Casimir-Polder-potential.

If the size of the periodic box is much larger than the finite range of the potential, one can simply extend the integration limits to the full plane,

$$\begin{aligned} V(q) &= \sum_{n=n_m}^{\infty} C_n \int_R^{\infty} \int_0^{2\pi} d\rho d\varphi \frac{e^{-iq\rho \cos\varphi}}{\rho^{n-1}} \\ &= 2\pi \sum_{n=n_m}^{\infty} \frac{C_n}{R^{n-2}} V_n(qR). \end{aligned} \quad (15)$$

By defining a dimensionless wave number $\bar{q} = qR$, the expression

$$V_n(\bar{q}) = \frac{{}_1F_2\left(1 - \frac{n}{2}; \left\{1, 2 - \frac{n}{2}\right\}; -\frac{\bar{q}^2}{4}\right)}{n-2} - \frac{n\Gamma\left(-\frac{n}{2}\right)}{2^n\Gamma\left(\frac{n}{2}\right)} \bar{q}^{n-2} \quad (16)$$

for the partial potential amplitudes is formed with the generalized hypergeometric function ${}_1F_2(a_1; \{b_1, b_2\}; z)$, as well as the gamma function $\Gamma(z)$ [48].

For each positive integer n this function can be represented explicitly in terms of Bessel functions. In Fig. 1, we depict the behavior of the potential amplitude $V_n(\bar{q})$ in its dependence on the dimensionless momentum \bar{q} for the powers $n = 3-7$. We notice the typical oscillatory Bessel-like behavior with a weak dependence on n .

In order to obtain the interaction energy between atoms and the tube, we have to sum the Casimir-Polder potential, weighed by the atomic density, over all space and over the whole length of the tube, leading to the expression

$$\hat{H}_i \equiv \int_0^L \frac{dz'}{L} \int_{\mathcal{V}} d^3r \hat{n}(\mathbf{r}) V[\hat{\mathbf{u}}(z') - \mathbf{r}]. \quad (17)$$

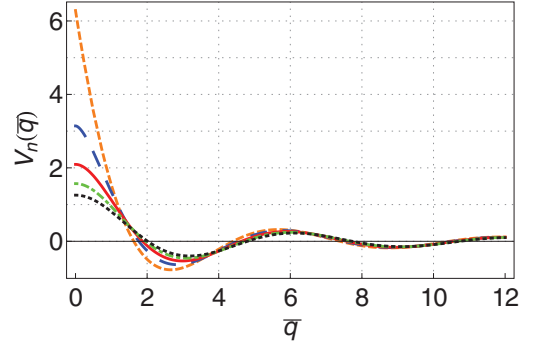


FIG. 1. (Color online) Dimensionless Fourier amplitudes $V_n(\bar{q})$ of the Casimir-Polder potential vs the dimensionless wave number \bar{q} for different inverse power laws: $n = 3$ (short-dashed orange line), $n = 4$ (long-dashed blue line), $n = 5$ (solid red line), $n = 6$ (dot-dashed green line), and $n = 7$ (dotted black line).

We note that \hat{H}_i is given by a convolution integral. For computational purposes, it is more convenient to transform it into the Fourier domain, where it becomes a separable sum of products of atomic and tube variables. Indeed, by introducing the atomic density fluctuations $\hat{\mathcal{N}}_q$ as the Fourier transform,

$$\hat{\mathcal{N}}_q \equiv \sqrt{\mathcal{V}} \int_{\mathcal{V}} d^3r \langle \mathbf{q} | \mathbf{r} \rangle \hat{n}(\mathbf{r}) = \sum_{\mathbf{k}} \hat{a}_{\mathbf{k}-q}^\dagger \hat{a}_{\mathbf{k}} = \hat{\mathcal{N}}_{-q}^\dagger, \quad (18)$$

of the atomic density and a translation operator,

$$\hat{\mathcal{T}}_q \equiv \int_0^L \frac{dz}{L} \exp[i\mathbf{q} \cdot \hat{\mathbf{u}}(z)], \quad (19)$$

of the tube, we can express the interaction energy as

$$\hat{H}_i \equiv \hbar \sum_{\mathbf{q}} w_{\mathbf{q}} \hat{\mathcal{N}}_{\mathbf{q}} \hat{\mathcal{T}}_{\mathbf{q}}. \quad (20)$$

Here, we have defined the frequency $w_{\mathbf{q}} \equiv V_{\mathbf{q}}/\hbar\sqrt{\mathcal{V}}$ to measure the strength of the Casimir-Polder potential.

D. Total energy

Therefore, the total Hamiltonian

$$\hat{H} \equiv \hat{H}_c + \hat{H}_a + \hat{H}_i \quad (21)$$

of the system is the sum of the phonon energy \hat{H}_c , the atomic kinetic energy \hat{H}_a , and the atom-phonon interaction energy \hat{H}_i .

Recalling the interaction energy equation (20), we notice that the homogeneous background contribution at $\mathbf{q} = 0$, depends only on the atomic particle number $\hat{N} \equiv \hat{\mathcal{N}}_0$. Hence, it is convenient to shift the individual energies by this amount, that is,

$$\hat{H}_i \rightarrow \hat{H}_i - \hbar w_0 \hat{N} = \sum_{\mathbf{q} \neq 0} \hbar w_{\mathbf{q}} \hat{\mathcal{N}}_{\mathbf{q}} \hat{\mathcal{T}}_{\mathbf{q}}, \quad (22)$$

$$\hat{H}_a \rightarrow \hat{H}_a + \hbar w_0 \hat{N} = \sum_{\mathbf{k}} (\varepsilon_{\mathbf{k}} + \hbar w_0) \hat{a}_{\mathbf{k}}^\dagger \hat{a}_{\mathbf{k}}. \quad (23)$$

This energy renormalization amounts to dropping the term $\mathbf{q} = 0$ in the interaction and offsetting the atomic dispersion relation by $\varepsilon_{\mathbf{k}} \rightarrow \varepsilon_{\mathbf{k}} + \hbar w_0$.

Experimentally relevant temperature scales are given by the cryogenically cooled atom chip, on which the carbon nanotube

is mounted, corresponding to $T_c = 4$ K, and by the temperature $T_a = 100$ nK of the atomic gas.

In Appendix A and Ref. [27], the maximal thermal displacement u of the tube as a function of temperature is estimated. Clearly, u decreases as the temperature of the chip decreases. On the other hand, the thermal de Broglie wavelength λ_{dB} of the atomic gas increases at lower temperatures. Hence, if we are in a regime where $u \ll \lambda_{dB}$, we can approximate the tube's displacement operator,

$$\hat{\mathcal{T}}_{\mathbf{q}} = 1 + \int_0^L \frac{dz}{L} \left\{ i\mathbf{q} \cdot \hat{\mathbf{u}}(z) - \frac{1}{2}[\mathbf{q} \cdot \hat{\mathbf{u}}(z)]^2 + \dots \right\}, \quad (24)$$

by the first two terms of the Taylor series of Eq. (19).

III. STATIC RELAXATION RATE

We are now ready to proceed with the calculation of the static relaxation rate using first-order time-dependent perturbation theory. From the solution of the Heisenberg equations for the phononic fields, we can derive the time-dependent occupation number of the lowest phononic mode. Then, we use Fermi's golden rule [49] to calculate the relaxation rate as a function of the temperature of the atomic gas. Our analysis demonstrates the possibility of carbon nanotube cooling in the experiment.

A. Heisenberg equations of motion

By evaluating the Heisenberg equations of motion for the atomic and phononic fields, i.e., $i\hbar\hat{A}(t) = [\hat{A}, \hat{H}]$, we obtain

$$\begin{aligned} \dot{\hat{a}}_{\mathbf{k}} = & -i\omega_{\mathbf{k}}\hat{a}_{\mathbf{k}} + \sum_{\mathbf{q} \neq 0} \sum_{\sigma=x,y} w_{\mathbf{q}} \mathbf{q} \cdot \mathbf{e}_{\sigma} \hat{a}_{\mathbf{k}+\mathbf{q}} \sum_{l=0}^{\infty} \left\{ I_l (\hat{b}_{l\sigma} + \hat{b}_{l\sigma}^{\dagger}) \right. \\ & \left. + iJ_l \sum_{\sigma'=x,y} \mathbf{q} \cdot \mathbf{e}_{\sigma'} (\hat{b}_{l\sigma} \hat{b}_{l\sigma'} + \hat{b}_{l\sigma}^{\dagger} \hat{b}_{l\sigma'}^{\dagger} + \hat{b}_{l\sigma} \hat{b}_{l\sigma'}^{\dagger} + \hat{b}_{l\sigma}^{\dagger} \hat{b}_{l\sigma'}^{\dagger}) \right\} \end{aligned} \quad (25)$$

and

$$\begin{aligned} \dot{\hat{b}}_{l\sigma} = & -i\omega_l \hat{b}_{l\sigma} + \sum_{\mathbf{q} \neq 0} w_{\mathbf{q}} \mathbf{q} \cdot \mathbf{e}_{\sigma} \hat{\mathcal{N}}_{\mathbf{q}} \\ & \times \left\{ I_l + 2iJ_l \sum_{\sigma'=x,y} \mathbf{q} \cdot \mathbf{e}_{\sigma'} (\hat{b}_{l\sigma'} + \hat{b}_{l\sigma'}^{\dagger}) \right\}, \end{aligned} \quad (26)$$

where the constants $I_l \equiv \int_0^L dz \phi_l(z)/\sqrt{2}L$ and $J_l \equiv a_l^2/4$ reflect the spatial extent of the l th phononic mode.

From the formal solution of Eq. (25) for the atomic variables, we obtain

$$\hat{a}_{\mathbf{k}}(t) = e^{-i\omega_{\mathbf{k}}t} \hat{a}_{\mathbf{k}}(0) + O(w), \quad (27)$$

which is a free evolution of the atomic field plus corrections.

First, we are only considering the two lowest degenerate phononic modes with $l = 0$. Excited-state modes with $l > 0$ will contribute little to the collisionally induced excitation rate considering the principle of energy conservation.

The two ground-state modes can be combined into a vector,

$$\hat{\mathbf{b}}_0(t) \equiv \sum_{\sigma=x,y} \hat{b}_{0\sigma}(t) \mathbf{e}_{\sigma}. \quad (28)$$

Within the rotating-wave approximation, we drop the counterrotating term in Eq. (26) and obtain a Langevin equation,

$$\dot{\hat{\mathbf{b}}}_0 = -i[\omega_0 - \hat{\Omega}(t)]\hat{\mathbf{b}}_0 + \hat{\mathbf{F}}(t), \quad (29)$$

for the phononic Kubo oscillators with a Hermitian frequency tensor,

$$\hat{\Omega}(t) = 2J_0 \sum_{\mathbf{q} \neq 0} w_{\mathbf{q}} (\mathbf{q} \otimes \mathbf{q})_{xy} \hat{\mathcal{N}}_{\mathbf{q}}(t), \quad (30)$$

which results in pressure-broadened oscillation frequencies and a stochastic force,

$$\hat{\mathbf{F}}(t) \equiv I_0 \sum_{\mathbf{q} \neq 0} w_{\mathbf{q}} \mathbf{q} \hat{\mathcal{N}}_{\mathbf{q}}(t). \quad (31)$$

The linear inhomogeneous Kubo equation (29) can be solved formally as

$$\hat{\mathbf{b}}_0(t) = \hat{U}_{\Omega}(t,0)\hat{\mathbf{b}}_0(0) + \int_0^t dt_1 \hat{U}_{\Omega}(t,t_1)\hat{\mathbf{F}}(t_1) \quad (32)$$

by introducing the retarded propagator

$$\partial_t \hat{U}_{\Omega}(t,t_1) = -i[\omega_0 - \hat{\Omega}(t)]\hat{U}_{\Omega}(t,t_1) \quad (33)$$

for times $t \geq t_1$, with the initial condition $\hat{U}_{\Omega}(t,t) = \mathbb{1}$. Thus, we have obtained a linear-response model for the carbon nanotube immersed in an atomic gas.

B. Occupation number

In this section, we assume that the state $\hat{\rho}_{\text{tot}} \equiv \hat{\rho}_a \otimes \hat{\rho}_c$ of atoms and phonons is initially uncorrelated. Furthermore, we consider atoms that are prepared in a grand-canonical ensemble $\hat{\rho}_a$ at a temperature $T_a \equiv 1/k_B\beta_a$ without macroscopic motion. Then, the number of the atoms with wave number \mathbf{k} is given by

$$n_{\mathbf{k}} \equiv \langle \hat{a}_{\mathbf{k}}^{\dagger} \hat{a}_{\mathbf{k}} \rangle = \frac{1}{e^{\beta_a(\epsilon_{\mathbf{k}} - \mu)} - 1}, \quad (34)$$

where we have introduced the chemical potential μ , or, alternatively, the fugacity $\eta \equiv e^{\beta_a\mu}$, to constrain the particle number to N as shown in Appendix B.

Moreover, the tube is prepared in its phononic vacuum $\hat{\rho}_c \equiv |0,0\rangle\langle 0,0|$, representing the ground state for the x and y polarization of the $l = 0$ modes.

As an observable, we consider the unpolarized occupation

$$p_0^v(t) \equiv \langle \hat{\mathbf{b}}_0^{\dagger}(t) \hat{\mathbf{b}}_0(t) \rangle = \text{Tr}\{\hat{\mathbf{b}}_0^{\dagger}(t) \hat{\mathbf{b}}_0(t) \hat{\rho}_{\text{tot}}\} \quad (35)$$

of the degenerate ground-state manifold. From Eq. (32), it follows that the occupation

$$\begin{aligned} p_0^v(t) = & \int_0^t dt_1 \int_0^{t_1} dt_2 \langle \hat{\mathbf{F}}^{\dagger}(t_1) \hat{U}_{\Omega}^{\dagger}(t,t_1) \hat{U}_{\Omega}(t,t_2) \hat{\mathbf{F}}(t_2) \rangle \\ = & \int_0^t dt_1 \int_0^{t_1} dt_2 e^{i\omega_0(t_2-t_1)} \langle \hat{\mathbf{F}}^{\dagger}(t_1) \hat{\mathbf{F}}(t_2) \rangle + O(w^3) \end{aligned} \quad (36)$$

is determined solely by the force-correlation function. In the evaluation of Eq. (36), we have used the Born approximation, keeping only processes up to second order in the Casimir-Polder potential amplitude $w_{\mathbf{q}}$. In turn, the force-correlation

function depends fundamentally on the density-correlation function $\langle \hat{N}_q(t_1) \hat{N}_k(t_2) \rangle$, which by means of space-time Fourier transformation is linked to the dynamic structure factor [50]. For the free fields of Eq. (27), we have evaluated this finite-temperature correlation function in Appendix B2.

After performing the time integration, we obtain for the occupation the second-order perturbative result,

$$p_0^v(t) = 4I_0^2 \sum_{\mathbf{q} \neq 0, \mathbf{k}} q_{\perp}^2 |w_{\mathbf{q}}|^2 n_{\mathbf{k}} (1 + n_{\mathbf{k}-\mathbf{q}}) \frac{\sin^2 \left[\Delta_{\mathbf{qk}} \frac{t}{2} \right]}{\Delta_{\mathbf{qk}}^2}. \quad (37)$$

Here, we have introduced the wave vector \mathbf{q}_{\perp} perpendicular to the tube axis by the relation $q_{\perp}^2 = q_x^2 + q_y^2$ and the frequency difference $\Delta_{\mathbf{qk}} \equiv \omega_0 + \omega_{\mathbf{k}-\mathbf{q}} - \omega_{\mathbf{k}}$ due to inelastic scattering between the initial and final states.

Assuming that the temperature T_a of the gas is above the temperature T_{BEC} for Bose-Einstein condensation, that is, $T_a > T_{\text{BEC}}$, the thermal occupation satisfies the inequality $n_{\mathbf{k}-\mathbf{q}} < 1$. Consequently, we can disregard this bosonic enhancement of scattering in Eq. (37) and retain only

$$p_0^v(t) \approx 4I_0^2 \sum_{\mathbf{q} \neq 0, \mathbf{k}} q_{\perp}^2 |w_{\mathbf{q}}|^2 n_{\mathbf{k}} \frac{\sin^2 \left[\Delta_{\mathbf{qk}} \frac{t}{2} \right]}{\Delta_{\mathbf{qk}}^2}. \quad (38)$$

Now, we evaluate the occupation number in the continuum limit $\sum_{\mathbf{k}} \rightarrow \int d^3k \mathcal{V}/(2\pi)^3$ and transform the \mathbf{k} integral to cylindrical coordinates (k, ϕ, k_z) with the k_z axis aligned to \mathbf{q} , which yields

$$p_0^v(t) = -\frac{mI_0^2 \mathcal{V}}{\pi^2 \hbar^2 \beta_a} \sum_{\mathbf{q} \neq 0} q_{\perp}^2 |w_{\mathbf{q}}|^2 \times \int_{-\infty}^{\infty} dk_z \ln \left(1 - \eta e^{-\beta_a \frac{\hbar^2 k_z^2}{2m}} \right) \frac{\sin^2 \left[\Delta_{\mathbf{qk}} \frac{t}{2} \right]}{\Delta_{\mathbf{qk}}^2}, \quad (39)$$

with $\Delta_{\mathbf{qk}} \equiv \omega_0 + \omega_q - \hbar q k_z / m$ and $q \equiv \sqrt{q_{\perp}^2 + q_z^2}$.

For an atomic gas at a temperature $T_a > T_{\text{BEC}}$, the fugacity obeys the inequality $\eta < 1$. Hence, we can Taylor expand the logarithm in Eq. (39) and arrive at

$$p_0^v(t) = \frac{m^2 I_0^2 \mathcal{V}}{\pi^2 \hbar^3 \beta_a} \sum_{j=1}^{\infty} \frac{\eta^j}{j} \sum_{\mathbf{q} \neq 0} \frac{q_{\perp}^2 |w_{\mathbf{q}}|^2}{q} \mathcal{F}_j(q), \quad (40)$$

where we have introduced the convolution integral

$$\mathcal{F}_j(q) \equiv \int_{-\infty}^{\infty} d\Delta \frac{\sin^2 \left[\Delta \frac{t}{2} \right]}{\Delta^2} e^{-j \frac{\beta_a \hbar}{4\omega_q} (\omega_0 + \omega_q - \Delta)^2}. \quad (41)$$

Integrals of this type are the essence of Fermi's golden rule [51]. If either the width $q/\sqrt{j\beta_a m}$ of the thermal Gaussian or its central frequency $\omega_0 + \omega_q$ is far larger than the width $2\pi/t$ of the sinc function localized at $\Delta = 0$, i.e., $t \gg \min(\sqrt{j\beta_a m}/q, 2\pi/\omega_0)$, then we can approximate the integral by evaluating the Gaussian function at the maximum of the sinc function as

$$\begin{aligned} \mathcal{F}_j(q) &\approx e^{-j \frac{\beta_a \hbar}{4\omega_q} (\omega_0 + \omega_q)^2} \int_{-\infty}^{\infty} d\Delta \frac{\sin^2 \left[\Delta \frac{t}{2} \right]}{\Delta^2} \\ &= t \frac{\pi}{2} e^{-j \frac{\beta_a \hbar}{4\omega_q} (\omega_0 + \omega_q)^2}. \end{aligned} \quad (42)$$

This expression displays the familiar linear increase of the excitation as a function of time.

C. Relaxation rate

The evaluation of relaxation rates is always based on time-dependent perturbation theory, either in the Schrödinger or in the Heisenberg picture, and a subsequent evaluation of the amount of excitation observed after turning on the interaction for some time. The linear temporal increase of the excitation then translates into a rate coefficient.

1. General expression

Substituting Eq. (42) into Eq. (40) and taking the time derivative at the initial instant, $\Gamma_0^v \equiv \dot{p}_0^v(t=0)$, we obtain the excitation rate,

$$\Gamma_0^v = \frac{m^2 I_0^2 L}{4\pi^2 \hbar^5 \beta_a} \sum_{j=1}^{\infty} \frac{\eta^j}{j} \int_0^{\infty} dq q^2 |V(q)|^2 e^{-j \frac{\beta_a \hbar}{4\omega_q} (\omega_0 + \omega_q)^2}. \quad (43)$$

We note the reappearance of the two-dimensional Fourier transform of the Casimir-Polder potential [Eq. (15)], depicted in Fig. 1.

In terms of the dimensionless wave number $\bar{q} = qR$ of Eq. (15), we can rewrite Eq. (43) as

$$\Gamma_0^v = \mathcal{A}_0 \sum_{j=1}^{\infty} \frac{\eta^j}{j} \int_0^{\infty} d\bar{q} |V(\bar{q})|^2 \delta_j^{(0)}(\bar{q}). \quad (44)$$

Here, we gathered all the constants into the prefactor $\mathcal{A}_l \equiv 8\pi m I_l^2 L / \hbar^3 \lambda_{\text{dB}}^5$ and introduced the sharply peaked function

$$\delta_j^{(l)}(\bar{q}) = \frac{4\bar{q}^2}{\sqrt{\pi} \varkappa^3} \exp \left[-j \left(\frac{\bar{q}}{\varkappa} + \frac{\varkappa \hbar \omega_l \beta_a}{\bar{q}} \right)^2 \right], \quad (45)$$

which depends on the characteristic ratio $\varkappa \equiv 4\sqrt{\pi} R / \lambda_{\text{dB}}$ of the tube's radius R to the thermal de Broglie wavelength $\lambda_{\text{dB}} \equiv \hbar \sqrt{2\pi \beta_a / m}$.

Indeed, $\delta_j^{(l)}(\bar{q})$ decreases very rapidly as $\bar{q} \rightarrow 0$ as well as for $\bar{q} \rightarrow \infty$, and we will treat it like a δ distribution compared to the smooth potential in the integral of Eq. (44). We can determine its extremum from $\partial_{\bar{q}} \delta_j^{(l)}(\bar{q}) = 0$ and find its location at

$$\bar{q}_j^{(l)} = \frac{\varkappa}{\sqrt{2j}} \{ 1 + [1 + (j\hbar \omega_l \beta_a / 2)^2]^{1/2} \}^{1/2}. \quad (46)$$

Therefore, we approximate the integral of Eq. (44) with the mean value theorem of integral calculus,

$$\int_0^{\infty} d\bar{q} |V(\bar{q})|^2 \delta_j^{(0)}(\bar{q}) \approx |V(\bar{q}_j^{(0)})|^2 \int_0^{\infty} d\bar{q} \delta_j^{(0)}(\bar{q}), \quad (47)$$

which, with the help of the known integral formula [48]

$$\int_0^{\infty} d\bar{q} \delta_j^{(0)}(\bar{q}) = \frac{e^{-j\hbar \omega_0 \beta_a}}{j^{3/2}} \left(1 + \frac{j}{2} \hbar \omega_0 \beta_a \right), \quad (48)$$

finally yields the excitation rate

$$\Gamma_0^v = \mathcal{A}_0 \sum_{j=1}^{\infty} \frac{e^{j\beta_a(\mu - \hbar \omega_0)}}{j^{5/2}} \left(1 + \frac{j}{2} \hbar \omega_0 \beta_a \right) |V(\bar{q}_j^{(0)})|^2. \quad (49)$$

Clearly, the first $j = 1$ term dominates the sum.

2. Fermi's golden rule

A simple view of the previous result comes from considering the unpolarized total transition rate

$$\Gamma_0^v = \sum_{k_f, \sigma_f} \sum_{k_i} \frac{2\pi}{\hbar} |\langle f | \hat{H}_i | i \rangle|^2 \delta(\varepsilon_f - \varepsilon_i) n_{k_i} \quad (50)$$

for the inelastic process induced by the Casimir-Polder potential of Eq. (22). This expression represents the signal current of a fictitious detector that records all final states of the atoms and averages it with the thermal distribution of initial states. Here, the initial state $|i\rangle = |1_{k_i}, 0_{\sigma_i}\rangle$ describes a single atom with wave vector k_i and the carbon nanotube in its ground state. This state has an energy $\varepsilon_i = \frac{\hbar^2}{2m} k_i^2$. As we are interested in inelastic collisions, we consider the final state $|f\rangle = |1_{k_f}, 1_{\sigma_f}\rangle$ with one phonon in the σ -polarized mode ω_0 . This state has an energy $\varepsilon_f = \hbar\omega_0 + \frac{\hbar^2}{2m} k_f^2$. With a few algebraic transformations, we obtain the excitation rate from Fermi's golden rule, and it coincides with the first term $j = 1$ of Eq. (49),

$$\Gamma_0^v = \frac{8\pi m I_0^2 L}{\hbar^3 \lambda_{\text{dB}}^5} e^{\beta_a(\mu - \hbar\omega_0)} \left(1 + \frac{1}{2} \hbar\omega_0 \beta_a\right) |V(\bar{q}_1^{(0)})|^2. \quad (51)$$

In order to bring out the essential physics, one can approximate the fugacity by $e^{\beta_a \mu} \approx n \lambda_{\text{dB}}^3$ for temperatures $T_a > T_{\text{BEC}}$ [compare to Eq. (B3)]. This simplifies the rate to

$$\Gamma_0^v = \frac{4m^2 I_0^2 L}{\hbar^5} \left(k_B T_a + \frac{1}{2} \hbar\omega_0\right) n e^{-\frac{\hbar\omega_0}{k_B T_a}} |V(\bar{q}_1^{(0)})|^2. \quad (52)$$

Thus, decreasing the thermal energy of the atoms below the excitation energy, i.e., $k_B T_a < \hbar\omega_0$, suppresses the inelastic relaxation rate exponentially.

3. Application to current experiment

In order to evaluate the relaxation rate Eq. (49) explicitly, we need to know the exact form of the Casimir-Polder potential of Eq. (15). Recent measurements of the interaction potential between the carbon nanotube and the atomic gas [29] have shown that the effect is very well described by the contribution C_5/ρ^5 with a numerical coefficient $C_5 \equiv 6 \times 10^{-65 \pm 1} \text{ J m}^5$. Thus, we approximate the Casimir-Polder potential Eq. (15) only by that term, i.e.,

$$V(\bar{q}_1^{(0)}) = 2\pi C_5 \frac{V_5(\bar{q}_1^{(0)})}{R^3}, \quad (53)$$

and $V_5(\bar{q}) = \frac{\bar{q}^3}{9} + \frac{1}{3} {}_1F_2(-\frac{3}{2}; \{1, -\frac{1}{2}\}; -\frac{\bar{q}^2}{4}) \approx \frac{1}{3} - \frac{\bar{q}^2}{4} + O[\bar{q}^3]$. As $R \ll \lambda_{\text{dB}}$, we need to retain only the lowest term in this expression and find the following approximation for the rate:

$$\Gamma_0^v = \frac{16\pi^2 m^2 I_0^2 L}{9\hbar^5} \left(k_B T_a + \frac{1}{2} \hbar\omega_0\right) n e^{-\frac{\hbar\omega_0}{k_B T_a}} \frac{C_5^2}{R^6}. \quad (54)$$

All other relevant parameters of the carbon nanotube and the atomic gas are listed in Appendices A and B.

Figure 2 depicts the dependence of the full excitation rate Γ_0^v of Eq. (49) on the scaled temperature T_a/T_{BEC} of the atomic cloud for different atomic densities. We note that the excitation rate depends strongly on the temperature, as well as on the

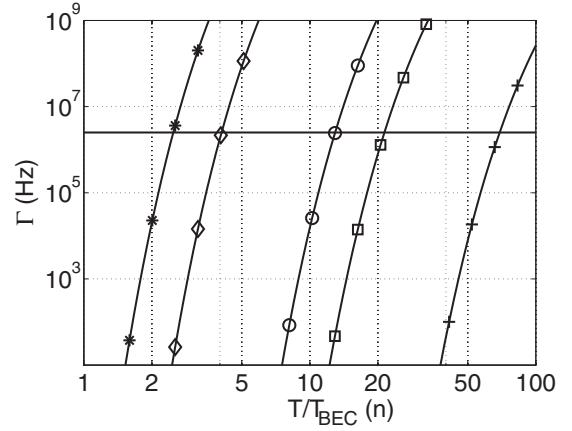


FIG. 2. Excitation rate Γ_0^v vs scaled temperature $T/T_{\text{BEC}}(n)$ for different densities n of the atomic cloud: $n = 10^{12} \text{ cm}^{-3}$ (crosses), $5 \times 10^{12} \text{ cm}^{-3}$ (squares), 10^{13} cm^{-3} (circles), $5 \times 10^{13} \text{ cm}^{-3}$ (diamonds), and 10^{14} cm^{-3} (stars). The horizontal line marks the frequency $\omega_0 = 2\pi \times 398 \text{ kHz}$ of the lowest phononic mode and represents the boundary between the overdamped (above) and the underdamped (below) oscillations of the carbon nanotube.

density of the gas. For the given parameters, we find the rates of Eqs. (49) and (54) are indistinguishable. When the excitation rates are of the order of the oscillation frequency or below $\Gamma_0^v < \omega_0$, the Fermi's golden rule approach is suitable. Therefore, we conclude that cooling the carbon nanotube to the ground mode is feasible in current experimental situations.

IV. DYNAMICS OF RELAXATION

In this section, we will generalize the previous considerations to determine the relevant time scales and study the dynamics of the relaxation process with a master equation approach. Here, the phonons are considered as the system and the atoms are the bath. This analysis yields (i) a dynamic picture of the carbon nanotube cooling, (ii) its approach towards equilibrium, and (iii) its dependence on temperature.

A. Master equation

In the interaction picture, the time evolution of the total density operator $\hat{\rho}_{\text{tot}}$ of phonons and atoms is described by the von Neumann equation

$$\dot{\hat{\rho}}_{\text{tot}}(t) = \frac{1}{i\hbar} [\hat{H}_i(t), \hat{\rho}_{\text{tot}}(t)]. \quad (55)$$

As usual, the interaction picture is obtained from the Schrödinger picture using the free atom-phonon propagator $\hat{U}(t) \equiv \exp[-i(\hat{H}_a + \hat{H}_c)t/\hbar]$, which yields

$$\hat{\rho}_{\text{tot}}(t) \equiv \hat{U}^\dagger(t) \hat{\rho}_{\text{tot}}(t) \hat{U}(t), \quad (56)$$

$$\hat{H}_i(t) \equiv \hat{U}^\dagger(t) \hat{H}_i \hat{U}(t) = \hbar \sum_{q \neq 0} w_q \hat{N}_q(t) \hat{T}_q(t), \quad (57)$$

$$\hat{N}_q(t) = \sum_k e^{-i(\omega_k - \omega_{k-q})t} \hat{a}_{k-q}^\dagger \hat{a}_k, \quad (58)$$

$$\hat{T}_q(t) = \int_0^L \frac{dz}{L} \exp[iq\hat{\mathbf{u}}(z,t)], \quad (59)$$

and

$$\hat{\mathbf{u}}(z, t) = \frac{1}{\sqrt{2}} \sum_{\substack{l=0 \\ \sigma=x,y}}^{\infty} \mathbf{e}_{\sigma} \phi_l(z) (e^{-i\omega_l t} \hat{b}_{l\sigma} + e^{i\omega_l t} \hat{b}_{l\sigma}^{\dagger}). \quad (60)$$

To study the phonon dynamics $\hat{\rho}(t) \equiv \text{Tr}_a[\hat{\rho}_{\text{tot}}(t)]$, we have to average the state of the total system over the atomic bath. Considering the deviation $\Delta\hat{\rho}(t) \equiv \hat{\rho}(t + \Delta t) - \hat{\rho}(t)$ for a short time interval Δt , we find from an iterated formal solution of Eq. (55) the expression

$$\begin{aligned} \Delta\hat{\rho}(t) = & \frac{1}{i\hbar} \int_t^{t+\Delta t} dt_1 \text{Tr}_a\{[\hat{H}_i(t_1), \hat{\rho}_{\text{tot}}(t)]\} \\ & - \frac{1}{\hbar^2} \int_t^{t+\Delta t} dt_1 \int_t^{t_1} dt_2 \text{Tr}_a\{[\hat{H}_i(t_1), [\hat{H}_i(t_2), \hat{\rho}_{\text{tot}}(t_2)]]\}. \end{aligned} \quad (61)$$

Within the Born-Markov approximation [51], we derive a master equation for the coarse-grained rate of change $\Delta\hat{\rho}(t) \approx \Delta t \frac{d\hat{\rho}}{dt}$. For the particular atom-phonon interaction Hamiltonian given by Eq. (57), we obtain the master equation

$$\begin{aligned} \frac{d\hat{\rho}}{dt} = & \frac{\eta\mathcal{V}}{\lambda_{\text{dB}}^3} \int_0^{\infty} \frac{d\tau}{\Delta t} \int_t^{t+\Delta t} dt' \sum_{q \neq 0} |w_q|^2 e^{-i\omega_q \tau (1 - i\frac{\tau}{\hbar\beta_a})} \\ & \times [\hat{T}_q^{\dagger}(t' - \tau) \hat{\rho}(t) \hat{T}_q(t') - \hat{T}_q(t') \hat{T}_q^{\dagger}(t' - \tau) \hat{\rho}(t)] + \text{H.c.} \end{aligned} \quad (62)$$

In progressing from Eq. (61) to Eq. (62), we have not included linear contributions in the interaction as there is no deterministic motion. Moreover, in evaluating thermal contributions for $T_a > T_{\text{BEC}}$, we have retained only the dominant contributions and encountered the same thermal density-fluctuation correlation function $\langle \tilde{N}_q(t_1) \tilde{N}_k(t_2) \rangle$, as in Eq. (36) and discussed in Appendix B2. Since the thermal correlation functions also decay quickly, it is very well justified to extend the upper limit of the τ integration to infinity.

B. Ground-state excitation rate

As an application of this master equation, we consider a carbon nanotube that is initially in the multimode phononic vacuum $\hat{\rho}(t=0) \equiv |0, \dots\rangle \langle 0, \dots|$. Then, we immerse it into the bath of atoms at temperature T_a and observe the decrease of the ground-state occupation $\rho^v(t) \equiv \langle 0 | \hat{\rho}(t) | 0 \rangle$. In this case, the excitation rate into any available phononic mode $l \geq 0$ is given by

$$\begin{aligned} \Gamma^v = & \frac{\eta\mathcal{V}}{\lambda_{\text{dB}}^3} \int_0^{\infty} \frac{d\tau}{\Delta t} \int_0^{\Delta t} dt' \sum_{q \neq 0} |w_q|^2 e^{-i\omega_q \tau (1 - i\frac{\tau}{\hbar\beta_a})} \\ & \times \langle 0 | \hat{Q}_q(t', t' - \tau) | 0 \rangle + \text{H.c.}, \end{aligned} \quad (63)$$

$$\hat{Q}_q(t_1, t_2) \equiv \hat{T}_q(t_1) \hat{T}_q^{\dagger}(t_2) - \hat{T}_q^{\dagger}(t_2) | 0 \rangle \langle 0 | \hat{T}_q(t_1). \quad (64)$$

Clearly, the excitation rate is just the negative depletion rate of the ground-state occupation, i.e., $\Gamma^v \equiv -\dot{\rho}^v(t)$.

As in Sec. IID, we assume that the thermal de Broglie wavelength of the atomic gas is much longer than the tube's oscillation amplitude, that is, $\lambda_{\text{dB}} \gg u$. Hence, we can

approximate the translation operator of Eq. (59), as in Eq. (24), by a second-order Taylor series and find

$$\langle 0 | \hat{Q}_q(t', t' - \tau) | 0 \rangle = \sum_{\substack{l=0 \\ \sigma=x,y}}^{\infty} (q e_{\sigma})^2 I_l^2 e^{-i\omega_l \tau}. \quad (65)$$

After performing the time integrations and transforming the discrete wave-number sums in the continuum limit, we arrive, for the vacuum excitation rate, at

$$\Gamma^v = \sum_{l=0}^{\infty} \mathcal{A}_l \eta \int_0^{\infty} d\bar{q} |V(\bar{q})|^2 \delta_1^{(l)}(\bar{q}). \quad (66)$$

The \bar{q} integration is approximated in a way completely analogous to Eq. (47), and we obtain the expression

$$\Gamma^v = \sum_{l=0}^{\infty} \mathcal{A}_l e^{\beta_a(\mu - \hbar\omega_l)} \left(1 + \frac{1}{2} \beta_a \hbar\omega_l\right) |V(\bar{q}_1^{(l)})|^2 \quad (67)$$

for the phononic excitation rate out of the vacuum. Clearly, the sum in Eq. (67) is dominated by the contribution of the lowest phononic mode $l=0$, that is,

$$\Gamma_0^v \approx \mathcal{A}_0 e^{\beta_a(\mu - \hbar\omega_0)} \left(1 + \frac{1}{2} \beta_a \hbar\omega_0\right) |V(\bar{q}_1^{(0)})|^2. \quad (68)$$

This expression for the rate agrees with the first term of the extended thermal series [Eq. (49)].

C. Finite-temperature thermalization rate

In this section, we generalize the previous calculation by assuming that the carbon nanotube is initially close to a thermal state at temperature $T_c \equiv 1/k_B \beta_c$, which is different from the temperature $T_a \equiv 1/k_B \beta_a$ of the atomic bath. The rate of change of the occupation $p_{l,\sigma} \equiv \langle \hat{p}_{l,\sigma} \rangle = \langle \hat{b}_{l,\sigma}^{\dagger} \hat{b}_{l,\sigma} \rangle$ of the mode (l, σ) is given by

$$\dot{p}_{l,\sigma} = \text{Tr}\{\hat{p}_{l,\sigma} \dot{\hat{\rho}}(t)\}. \quad (69)$$

Now, we use the master equation (62) and assume in the evaluation of the averages a canonical density operator parametrized by a time-dependent coefficient $\beta_c(t)$, as outlined in Appendix B3. In the continuum limit, we obtain from Eq. (69) for the unpolarized occupation numbers $p_l \equiv p_{l,x} + p_{l,y}$ of the l th level the rate equation

$$\dot{p}_l(t) = -\gamma_l(\beta_c) p_l, \quad (70)$$

with temperature-dependent rate coefficients

$$\gamma_l(\beta_c) \equiv \mathcal{A}_l \eta (e^{\beta_a \hbar\omega_l} - e^{\beta_c \hbar\omega_l}) \int_0^{\infty} d\bar{q} |V(\bar{q})|^2 \delta_1^{(l)}(\bar{q}). \quad (71)$$

Integrating over \bar{q} similarly to Eqs. (44) and (47), we find

$$\gamma_l = \mathcal{A}_l \eta \left(1 - e^{(\beta_c - \beta_a) \hbar\omega_l}\right) \left(1 + \frac{\beta_a \hbar\omega_l}{2}\right) |V(\bar{q}_1^{(l)})|^2, \quad (72)$$

with $\bar{q}_1^{(l)}$ given by Eq. (46).

As expected, this expression generalizes Eqs. (49) and (67), as it allows for a finite temperature of the tube that is different

from the atomic gas, i.e., $\beta_c \neq \beta_a$, as well as for excitations into all phononic modes $l \geq 0$.

If the carbon nanotube is hotter than the atomic bath, that is, $\beta_c < \beta_a$, then the relaxation rate of Eq. (72) is positive and leads, according to Eq. (70), to a cooling of the tube's phonons. If the carbon nanotube is colder than the atoms, i.e., $\beta_c > \beta_a$, the rate is negative and leads to a heating of the tube. Finally, all rates vanish, when $\beta_c = \beta_a$, as required for a thermodynamic equilibrium.

V. CONCLUSION

Using time-dependent perturbation theory with finite-temperature ensembles, we have calculated the excitation rate of a free-standing single-walled carbon nanotube immersed in a bath of neutral bosonic atoms. The interaction between the carbon nanotube and the atoms was modeled by a generic Casimir-Polder potential series. We have assumed that the temperature of the atoms was above the Bose-Einstein condensation transition temperature as the collisional relaxation at the megahertz level is insensitive to the phase coherence of the bath.

For the numerical evaluation of the excitation rates, we have used experimentally determined values of the Casimir-Polder potential between a thermally and a Bose-Einstein condensed ^{87}Rb gas [29]. In this situation, an inverse power law $\sim C_5/r^5$ is very well suited to approximate this potential. With this analysis and the current data, we find that cooling of the free-standing carbon nanotube to the phononic ground state due to the Casimir-Polder interaction with a cold atomic gas is feasible.

We emphasize that the excitation rate depends strongly on the temperature and the density of the atomic cloud. The form of the interaction potential, for example, interferences between different potential contributions, can influence the rate as well. Hence, more extensive experimental data are needed.

ACKNOWLEDGMENTS

J.F. and C.T.W. gratefully acknowledge support from the German BMBF (NanoFutur 03X5506). W.P.S. and J.F. cooperated within the SFB/TRR 21 ‘‘Control of quantum correlations in tailored matter’’ funded by the Deutsche Forschungsgemeinschaft (DFG), and R.W. thanks the Deutsche Luft- und Raumfahrtagentur (DLR) for support from Grant No. 50WM 1137.

APPENDIX A: PROPERTIES OF THE CARBON NANOTUBE

In this Appendix, we summarize, without much of a derivation, properties of the carbon nanotube relevant for the article.

The normalization constant \tilde{a}_l of the eigenmode of Eq. (4) reads

$$\begin{aligned} \frac{\tilde{a}_l^2}{a_l^2} &= 1 + 2 \cos(\kappa_l L) \cosh(\kappa_l L) + \frac{1}{2} [\cos(2\kappa_l L) \\ &+ \cosh(2\kappa_l L)] - \frac{1}{2\kappa_l L} [2 \cosh(\kappa_l L) \sin(\kappa_l L) \\ &+ 2 \cos(\kappa_l L) \sinh(\kappa_l L) + \cosh^2(\kappa_l L) \sin(2\kappa_l L) \\ &+ \cos^2(\kappa_l L) \sinh(2\kappa_l L)]. \end{aligned} \quad (\text{A1})$$

TABLE I. Mechanical parameters of a single-walled carbon nanotube.

R (nm)	L (μm)	ρ_c (kg/m)	ω_0 (kHz)	a_0 (nm)
1	1	10^{-15}	$2\pi \times 398$	0.2

Typical mechanical parameters for a single-walled carbon nanotube are summarized in Table I.

In the low-temperature approximation of Eq. (24), we have assumed that the spatial excursions of the nanotube are much less than the thermal de Broglie wavelength of the atomic gas. Thus, we summarize [27] the maximal thermal excursions $u = \sqrt{\langle \Delta^2 \hat{u} \rangle_{T_c}}$ of the tip of the tube $z = L$ for different temperatures of the tube T_c in Table II.

APPENDIX B: COLD BOSONIC GASES

In this Appendix, we summarize the central results of equilibrium thermodynamics of bosonic fields that were employed in the main sections of the article.

1. Bose-Einstein condensation

The state of the free atomic gas [52] is described by the density operator of the grand-canonical ensemble,

$$\hat{\rho} = e^{\Omega - \beta_a(\hat{H} - \mu\hat{N})}, \quad \text{Tr}\{\hat{\rho}\} = 1, \quad (\text{B1})$$

held at a temperature $T_a \equiv 1/k_B\beta_a$ and maintaining an average particle number N . The Hamiltonian is denoted by \hat{H} , Ω is the grand-canonical potential, and μ is a chemical potential, which is determined self-consistently through the particle number constraint,

$$N \equiv \langle \hat{N} \rangle = \sum_k n_k = n_0 + \tilde{N}(\beta_a). \quad (\text{B2})$$

Here $n_0 \equiv n_{k=0}$ is the occupation of the ground state and $\tilde{N}(\beta_a)$ denotes the number of thermal particles.

Introducing the fugacity as $\eta \equiv e^{\beta_a\mu}$, one finds for the occupation number of the ground state $n_0 \equiv \eta/(1-\eta)$ and $\tilde{N}(\beta_a) = \mathcal{V}g_{3/2}(\eta)/\lambda_{\text{dB}}^3$ for the number of particles in the excited states. The polylogarithmic function is defined by

$$g_{3/2}(\eta) \equiv \sum_{j=1}^{\infty} \frac{\eta^j}{j^{3/2}}, \quad g_{3/2}(1) \approx 2.61238 \quad (\text{B3})$$

In the thermodynamical limit, when particle number and volume increase at constant particle density, i.e., $n = \lim_{N, \mathcal{V} \rightarrow \infty} N/\mathcal{V} = \text{const}$, one can identify two cases. The first corresponds to particle densities below the critical density, that is, $n < g_{3/2}(1)/\lambda_{\text{dB}}^3$. There, the occupation number of the ground state n_0 is negligibly small and the total number of atoms is equal to the number of particles in the excited states

TABLE II. Maximal thermal displacement u at the tip of the carbon nanotube for three values of temperature T_c .

T_c (K)	4	0.24	0
u (nm)	270	66	0.46

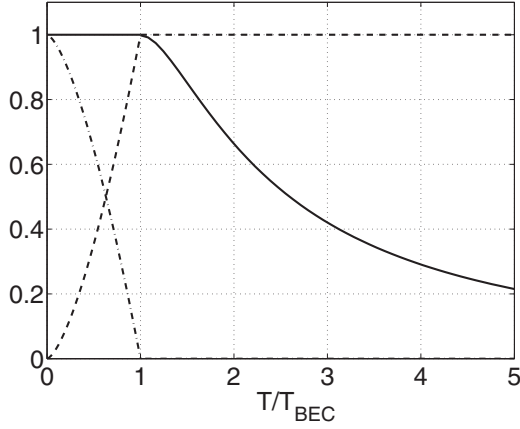


FIG. 3. Fugacity η as a function of scaled temperature T/T_{BEC} (solid line), fraction of particles in the ground state n_0/N (dash-dotted line), and fraction of particles in the excited states \tilde{N}/N (dashed line).

$N \approx \tilde{N}(\beta_a)$. In this limit of a dilute quantum gas, the de Broglie wavelength is much smaller than the average distance between the particles. Therefore, the gas behaves classically.

The second regime occurs for densities larger than the critical density $n > g_{3/2}(1)/\lambda_{\text{dB}}^3$. In this case the fugacity attains its maximum value $\eta \rightarrow 1$. The occupation of the ground state,

$$n_0 = N \left[1 - \left(\frac{T_a}{T_{\text{BEC}}} \right)^{3/2} \right], \quad (\text{B4})$$

is not negligible anymore and increases with the decrease of temperature where we have introduced the critical BEC temperature,

$$T_{\text{BEC}} \equiv \frac{2\pi\hbar^2}{mk_B} \left[\frac{n}{g_{3/2}(1)} \right]^{2/3}. \quad (\text{B5})$$

Figure 3 presents the behavior of the gas in these two cases. For temperatures below the critical temperature, the ground-state occupation (dash-dotted line) becomes macroscopic and the fugacity (solid line) is practically 1. Above the critical temperature, the fugacity decreases with the increase of temperature, and the number of particles in the excited states (dashed line) is equal to the total number of particles.

From this analysis, we can obtain the values of the thermal de Broglie wavelength, summarized in Table III, for a range of atomic densities at the critical temperature.

2. Thermal correlation functions

In this part of the Appendix we focus on the quantum averages used in the master equation (62). In particular,

TABLE III. Parameters of the cold atomic cloud. The mass of a single ^{87}Rb atom is $m = 1.443 \times 10^{-25}$ kg.

n (cm^{-3})	10^{12}	5×10^{12}	10^{13}	5×10^{13}	10^{14}
T_{BEC} (nK)	18	54	85	250	400
λ_{dB} (nm)	610	357	283	165	131

we derive single-time averages and two-time correlation functions.

a. Single-time average

With the choice of the interaction Hamiltonian (57) and assuming that the atomic bath is in a grand-canonical state without macroscopic motion, we find a vanishing quantum average

$$\text{Tr}_a \{ \hat{\rho}_a \hat{H}_i \} = 0 \quad (\text{B6})$$

because $\langle \hat{a}_{k-q}^\dagger \hat{a}_k \rangle = 0$ for $\mathbf{q} \neq 0$. Therefore, the trace over the single commutator in the first term of Eq. (61) will vanish, which means that we have incorporated this energy shift in the unperturbed Hamiltonian of the atoms. This result is well known in first-order time-independent perturbation theory.

b. Two-time correlations

The two-time density-fluctuation correlation function $\langle \hat{N}_q(t_1) \hat{N}_k(t_2) \rangle$ evaluated at temperature T_a emerges ubiquitously in field theory and is proportional to the dynamic structure factor [50]. In the case of stationary, translationally invariant systems, it simplifies to

$$\langle \hat{N}_q(t + \tau) \hat{N}_k(t) \rangle = \langle \hat{N}_q(\tau) \hat{N}_k(0) \rangle = \delta_{q+k,0} g_q(\tau),$$

where the Kronecker δ enforces momentum conservation, and we find the thermal correlation function

$$g_q(\tau) \equiv \sum_k e^{i(\omega_{k-q} - \omega_k)\tau} n_{k-q} (1 + n_k), \quad (\text{B7})$$

with thermal occupations n_k defined in Eq. (34).

For further discussions, we separate the ground-state contribution from the sum and approximate the remainder within the continuum-limit. For $T_a > T_{\text{BEC}}$, we find $n_k < 1$ and we will take only the linear term in Eq. (B7) into account. In this regime, we can also approximate the Bose-Einstein distribution by the Maxwell-Boltzmann distribution. Moreover, the occupation number in the lowest level is negligible and the correlation function can be written as

$$g_q(\tau) \approx \frac{\eta \mathcal{V}}{\lambda_{\text{dB}}^3} \exp \left[-i\omega_q \tau \left(1 - i \frac{\tau}{\hbar\beta_a} \right) \right]. \quad (\text{B8})$$

3. Canonical ensemble for phonons

In this section, we recall general properties of the canonical ensemble,

$$\hat{\rho}_c \equiv e^{\bar{\Omega} - \beta_c \hat{H}_c}, \quad \text{Tr}_c \{ \hat{\rho}_c \} = 1, \quad (\text{B9})$$

which is used when the system exchanges energy but no particles with the environment. Here, $\bar{\Omega}$ is a canonical potential, \hat{H}_c is the Hamiltonian defined by Eq. (9) for the phonons of the carbon nanotube, and $T_c \equiv 1/k_B\beta_c$ is the temperature of the phonons.

Therefore, the occupation of the mode (l, σ) reads

$$p_{l,\sigma}(\beta_c) \equiv \langle \hat{p}_{l,\sigma} \rangle = \frac{1}{e^{\beta_c \hbar \omega_l} - 1}, \quad (\text{B10})$$

and for the density correlation, we find

$$\langle \hat{p}_{l,\sigma} \hat{p}_{l',\sigma'} \rangle \equiv (1 + \delta_{l,l'} \delta_{\sigma,\sigma'} e^{\beta_c \hbar \omega_l}) p_{l,\sigma} p_{l',\sigma'}. \quad (\text{B11})$$

Recalling Eq. (62), we obtain from Eq. (B10) the rate of change

$$\begin{aligned} \dot{p}_{l,\sigma} = & \int_0^\infty \frac{d\tau}{\hbar^2 \Delta t} \int_t^{t+\Delta t} dt' \sum_{q \neq 0} \{g_q(\tau) [\langle \hat{T}_q(t') \hat{p}_{l,\sigma} \hat{T}_q^\dagger(t' - \tau) \rangle \\ & - \langle \hat{p}_{l,\sigma} \hat{T}_q(t') \hat{T}_q^\dagger(t' - \tau) \rangle] + \text{H.c.} \} \end{aligned} \quad (\text{B12})$$

of the occupation of mode (l, σ) .

With the quadratic approximation of the tube's translation operator Eq. (24), we find

$$\begin{aligned} & \langle \hat{p}_{l,\sigma} \hat{T}_q(t') \hat{T}_q^\dagger(t' - \tau) \rangle - \langle \hat{T}_q(t') \hat{p}_{l,\sigma} \hat{T}_q^\dagger(t' - \tau) \rangle \\ & = \sum_{l',\sigma'} I_{l',\sigma'}^2 (q e_{\sigma'})^2 \{ \langle \hat{p}_{l,\sigma} \rangle (e^{-i\omega_{l'}\tau} - e^{-\omega_{l'}(\beta_c \hbar - i\tau)}) \\ & + \langle \hat{p}_{l',\sigma'} \hat{p}_{l,\sigma} \rangle [2 \cos(\omega_{l'}\tau) - e^{\omega_{l'}(\beta_c \hbar - i\tau)} - e^{-\omega_{l'}(\beta_c \hbar - i\tau)}] \}. \end{aligned} \quad (\text{B13})$$

We note that these expressions are very similar to those considered in Sec. IV B for the ground-state excitation. Using Eqs. (B10) and (B11) and integrating over t' and τ , we obtain

$$\begin{aligned} \dot{p}_{l,\sigma}(\beta_c) = & \frac{\eta m \mathcal{V}}{\hbar \lambda_{\text{dB}}^2} \sum_{q \neq 0} \frac{|w_q|^2}{|q|} \sum_{l',\sigma'} I_{l',\sigma'}^2 (q e_{\sigma'})^2 e^{-\frac{\hbar \beta_c (\omega_q - \omega_{l'})^2}{4\omega_q}} \\ & \times (e^{-\beta_c \hbar \omega_{l'}} - e^{-\beta_c \hbar \omega_{l'}}) [1 + (1 + \delta_{l,l'} \delta_{\sigma,\sigma'} e^{\beta_c \hbar \omega_{l'}}) \\ & \times (1 - e^{\beta_c \hbar \omega_{l'}}) p_{l',\sigma'}(\beta_c)] p_{l,\sigma}(\beta_c). \end{aligned} \quad (\text{B14})$$

With the help of Eq. (B10), Eq. (B14) reduces to

$$\begin{aligned} \dot{p}_{l,\sigma}(\beta_c) = & \frac{\eta m \mathcal{V}}{\hbar \lambda_{\text{dB}}^2} \sum_{q \neq 0} \frac{|w_q|^2}{|q|} I_l^2 (q e_\sigma)^2 e^{-\frac{\hbar \beta_c (\omega_q - \omega_l)^2}{4\omega_q}} \\ & \times (e^{(\beta_c - \beta_a) \hbar \omega_l} - 1) p_{l,\sigma}(\beta_c). \end{aligned} \quad (\text{B15})$$

These technical steps are necessary to obtain the finite-temperature thermalization rate of Eq. (72).

-
- [1] R. P. Feynman, *J. Microelectromech. Syst.* **1**, 60 (1992).
- [2] B. Rodgers, S. Pennathur, and J. Adams, *Nanotechnology: Understanding Small Systems* (CRC Press, Boca Raton, FL, 2008).
- [3] M. Nielsen and I. Chuang, *Quantum Computation and Quantum Information* (Cambridge University Press, Cambridge, 2000).
- [4] M. Aspelmeyer, P. Meystre, and K. Schwab, *Phys. Today* **65**(7), 29 (2012).
- [5] G. Milburn and M. Woolley, *Acta Phys. Slovaca* **61**, 483 (2012).
- [6] L. Tian and P. Zoller, *Phys. Rev. Lett.* **93**, 266403 (2004).
- [7] S. Schmid, A. Härter, and J. H. Denschlag, *Phys. Rev. Lett.* **105**, 133202 (2010).
- [8] *Quantum Gases: Finite Temperature and Non-Equilibrium Dynamics*, edited by S. Gardiner, N. Proukakis, and M. Davis (Imperial College Press, London, 2013), and references therein.
- [9] M. Grupp, W. P. Schleich, E. Goldobin, D. Koelle, R. Kleiner, and R. Wälsler, *Phys. Rev. A* **87**, 021602 (2013), and references therein.
- [10] A. Recati, P. O. Fedichev, W. Zwerger, J. von Delft, and P. Zoller, *Phys. Rev. Lett.* **94**, 040404 (2005).
- [11] I. Wilson-Rae, P. Zoller, and A. Imamoglu, *Phys. Rev. Lett.* **92**, 075507 (2004).
- [12] J. Chan, T. P. Mayer Alegre, A. H. Safavi-Naeini, J. T. Hill, A. Krause, S. Groeblacher, M. Aspelmeyer, and O. Painter, *Nature (London)* **478**, 89 (2011).
- [13] M. Poot and H. S. J. van der Zant, *Phys. Rep.* **511**, 273 (2012).
- [14] I. B. Mekhov and H. Ritsch, *J. Phys. B* **45**, 102001 (2012).
- [15] E. Gavartin, P. Verlot, and T. J. Kippenberg, *Nat. Nanotechnol.* **7**, 509 (2012).
- [16] S. Machnes, J. Cerrillo, M. Aspelmeyer, W. Wieczorek, M. B. Plenio, and A. Retzker, *Phys. Rev. Lett.* **108**, 153601 (2012).
- [17] B. H. Schneider, S. Etaki, H. S. J. van der Zant, and G. A. Steele, *Sci. Rep.* **2**, 599 (2012).
- [18] D. Hunger, S. Camerer, T. W. Hänsch, D. König, J. P. Kotthaus, J. Reichel, and P. Treutlein, *Phys. Rev. Lett.* **104**, 143002 (2010).
- [19] G. Birkl and J. Fortágh, *Laser Photonics Rev.* **1**, 12 (2007).
- [20] B. I. Yakobson and R. E. Smalley, *Am. Sci.* **85**, 324 (1997).
- [21] R. Saito, G. Dresselhaus, and M. S. Dresselhaus, *Physical Properties of Carbon Nanotubes* (Imperial College Press, London, 1999).
- [22] H. W. Kroto, J. R. Heath, S. C. O'Brien, R. F. Curl, and R. E. Smalley, *Nature (London)* **318**, 162 (1985).
- [23] R. Folman, P. Krüger, J. Schmiedmayer, J. Denschlag, and C. Henkel, *Adv. At. Mol. Opt. Phys.* **48**, 263 (2002).
- [24] J. Fortágh and C. Zimmermann, *Science* **307**, 860 (2005).
- [25] J. Fortágh and C. Zimmermann, *Rev. Mod. Phys.* **79**, 235 (2007).
- [26] S. Zippilli, G. Morigi, and A. Bachtold, *Phys. Rev. Lett.* **102**, 096804 (2009).
- [27] C. T. Weiß, *Reversible Dynamics of Cold Quantum Gases and Irreversible Coupling to Carbon Nanotubes* (Dr. Hut Verlag, München, 2010).
- [28] A. Goodsell, T. Ristorph, J. A. Golovchenko, and L. V. Hau, *Phys. Rev. Lett.* **104**, 133002 (2010).
- [29] P. Schneeweiss, M. Gierling, G. Visanesu, D. P. Kern, T. E. Judd, A. Günther, and J. Fortágh, *Nat. Nanotechnol.* **7**, 515 (2012).
- [30] H. B. G. Casimir and D. Polder, *Phys. Rev.* **73**, 360 (1948).
- [31] S. K. Lamoreaux, *Phys. Today* **60**(2), 40 (2007).
- [32] G. L. Klimchitskaya, U. Mohideen, and V. M. Mostepanenko, *Rev. Mod. Phys.* **81**, 1827 (2009).
- [33] M. Antezza, L. P. Pitaevskii, and S. Stringari, *Phys. Rev. A* **70**, 053619 (2004).
- [34] D. M. Harber, J. M. Obrecht, J. M. McGuirk, and E. A. Cornell, *Phys. Rev. A* **72**, 033610 (2005).
- [35] J. M. Obrecht, R. J. Wild, M. Antezza, L. P. Pitaevskii, S. Stringari, and E. A. Cornell, *Phys. Rev. Lett.* **98**, 063201 (2007).
- [36] B. Jetter, J. Märkle, P. Schneeweiss, M. Gierling, S. Scheel, A. Günther, J. Fortágh, and T. E. Judd, *New J. Phys.* **15**, 073009 (2013).
- [37] R. Fermani, S. Scheel, and P. L. Knight, *Phys. Rev. A* **75**, 062905 (2007).
- [38] G. L. Klimchitskaya, E. V. Blagov, and V. M. Mostepanenko, *J. Phys. A* **41**, 164012 (2008).

- [39] M. Gierling, P. Schneeweiss, G. Visanescu, P. Federsel, M. Häffner, D. Kern, T. E. Judd, A. Günther, and J. Fortágh, *Nat. Nanotechnol.* **6**, 446 (2011).
- [40] L. D. Landau and E. M. Lifshitz, in *Elastizitätstheorie*, edited by P. Ziesche (Akademie, Berlin, 1991), Vol. VII.
- [41] D. Qian, G. J. Wagner, W. K. Liu, M.-F. Yu, and R. R. Ruoff, *Appl. Mech. Rev.* **55**, 495 (2002).
- [42] S. M. Han, H. Benaroya, and T. Wei, *J. Sound Vib.* **225**, 935 (1999).
- [43] D. Garcia-Sanchez, A. San Paulo, M. J. Esplandiu, F. Perez-Murano, L. Forró, A. Aguasca, and A. Bachtold, *Phys. Rev. Lett.* **99**, 085501 (2007).
- [44] M. S. Dresselhaus and P. C. Eklund, *Adv. Phys.* **49**, 705 (2000).
- [45] G. L. Klimchitskaya, E. V. Blagov, and V. M. Mostepanenko, *J. Phys. A* **39**, 6481 (2006).
- [46] E. V. Blagov, G. L. Klimchitskaya, and V. M. Mostepanenko, *Phys. Rev. B* **75**, 235413 (2007).
- [47] T. E. Judd, R. G. Scott, A. M. Martin, B. Kaczmarek, and T. M. Fromhold, *New J. Phys.* **13**, 083020 (2011).
- [48] I. S. Gradshteyn and I. M. Ryzhik, *Table of Integrals, Series and Products* (Academic, New York, 2000).
- [49] Correctly speaking, Fermi's golden rule should be attributed to P. A. M. Dirac, *Proc. R. Soc., Ser. A* **114**, 243 (1927); see T. D. Visser, *Am. J. Phys.* **77**, 487 (2009).
- [50] D. Pines, *Elementary Excitations in Solids* (Benjamin, New York, 1963).
- [51] C. Cohen-Tannoudji, J. Dupont-Roc, and G. Grynberg, *Atom-Photon Interaction* (Wiley, New York, 1992).
- [52] L. Pitaevskii and S. Stringari, *Bose-Einstein Condensation* (Oxford University Press, Oxford, 2003).